Stochastic Optimization for Power System Configuration with Renewable Energy in Remote Areas

Ludwig Kuznia[1], Bo Zeng[1], Grisselle Centeno[1] and Zhixin Miao[2]

[1] – Dept. of Industrial and Management Systems Engineering, Tampa, FL 33620
email: lkuznia@mail.usf.edu, {bzeng, gcenteno}@usf.edu
[2] – Dept. of Electrical Engineering, University of South Florida, Tampa, FL 33620
zmiao@usf.edu

February 17, 2011

Abstract

This paper presents the first stochastic mixed integer programming model for a comprehensive hybrid power system design, including renewable energy generation, storage device, transmission network, and thermal generators, in remote areas. Given the computational complexity of the model, we developed a Benders' decomposition algorithm with Pareto-optimal cuts. Computational results show significant improvement in our ability to solve this type of problem in comparison to a state-of-the-art professional solver. This model and the solution algorithm provide an analytical decision support tool for the hybrid power system design problem.

Keywords: stochastic mixed integer programming, power system design, renewable energy, Benders' decomposition

1 Introduction

Providing energy to remote or isolated areas can be extremely costly due to the investment associated with transmission networks, land acquisition, control towers, and construction materials. The issue of energy independence is also a concern given that traditional configurations of power delivery depend heavily on energy or fuel generated outside the target area. There are two typical ways to deliver energy to remote areas, through transmission lines from places with excess capacity or large-scale generating facilities, or by utilizing a local thermal generating facility. Establishing a line to an offshore island is very expensive due to the complications associated with laying underwater transmission lines. Power generation using local thermal systems can be even more expensive due to high transportation and inventory holding costs [7] [21] [22]. Moreover, both options unavoidably lead to environmental concerns, especially the latter which produces a large volume of green house gases and pollutants. Technology advancements, especially relating to wind and solar energy, provide remote areas with the option of renewable energy systems for reliable energy supply. Compared with traditional systems, renewable energy systems have a clear advantage environmentally as well as on the energy independence aspect.

In 2009, the American Clean Energy and Security Act of 2009 [10], was passed by the U.S. House of Representatives requiring the deployment of clean energy resources and a reduction in pollutants that contribute to global warming. This act will aid in the transition to a clean energy economy. However, the implementation of a reliable clean energy system may be limited by the nature of wind and solar energy which tends to be intermittent and highly variable [2] [21] [22]. To handle this challenge, energy storage equipment including pump water [6], battery [19], and hydrogen and a fuel cell [7], can be integrated into the system. Also, traditional thermal generators and transmission lines can be utilized, in a less frequent fashion, to deal with the random generation aspect of renewable energy/storage device systems, see [18] and references therein for a recent review.

Various heuristics have been applied to this problem, including simulated annealing [8], genetic algorithm [22], and tabu search [13], to derive good solutions. To capture the impact of randomness in system design, simulation based optimization methods are among the most popular approaches due to their ability to evaluate the system design in random environments, see [5] a review on simulation optimization study. One obvious drawback of heuristics and simulation based optimization is that they cannot guarantee the quality of the solution. Therefore, these methods yield little insight into optimal system configuration.

Stochastic programming models have also been applied to model the energy system design problem and to derive the optimal configuration considering various probabilistic scenarios. In [1], a stochastic mixed integer programming model for optimal sizing of storage system is developed for an existing isolated wind-diesel power system. The randomness for wind and load is described by a set of scenarios where one scenario represents a 24-hour instance of wind and load. The model is solved using a solver with GAMS [9]. In [6], a stochastic linear programming model is developed for optimal capacity design of a pumped storage device in a hybrid system where thermal generators' generation level is known. Nevertheless, with the exception of storage capacity, little work has been done using stochastic programming as a tool to study the larger scope design. This may be due to the limitation of solvers to efficiently deal with the complexity of the hybrid system design problem.

In this paper, we consider a hybrid system design problem for an isolated area, which depends on a local thermal generator and expects an increase in electric demand in the near future. The set of options considered for the configuration include building a long distance transmission network or constructing renewable energy facilities and a storage system as shown in Figure 1. For this problem, we build a stochastic mixed integer programming model to derive the optimal configuration with random renewable energy generation and demand. To address the computational challenges, we develop an algorithm using Benders' decomposition method that can efficiently solve practical system design problems. To our knowledge, this is the first time a stochastic discrete optimization model for comprehensive hybrid system design has been developed as well as the first effective computational tool.

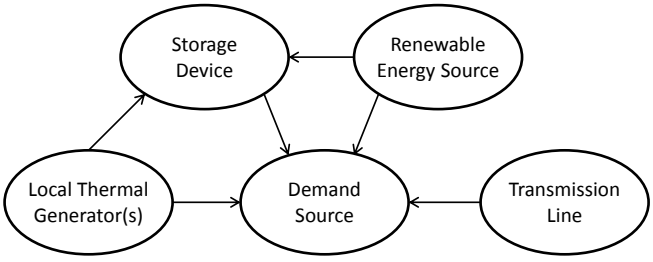

Figure 1: Transfer of Energy in a Hybrid System

The paper is organized as follows: In Section 2, the problem description and the mathematical formulation are provided. In Section 3, the details of the Benders' decomposition algorithm developed are presented. Section 4 provides the computational results for a set of test instances. Conclusions and future research directions are discussed in Section 5.

2 Problem Description and Mathematical Formulation

In this section, we first describe the modeling background in the hybrid system design. We then present the stochastic mixed integer programming model. Also, by observing this model is equivalent to capacitated lot-sizing problem under special circumstances, we show that this model is in general $\mathcal{NP}$-hard.

We consider the system design problem for a remote area which currently has a local thermal generator and must accommodate an increase in demand in the near future. Thus, installation and capacity decisions for the renewable energy generation (we will focus on wind generated energy, though the model is applicable to other forms of renewable energy as well), the storage device, and/or the transmission network must be made. In our study, as we focus on the long-term system configuration, we do not model the local generator's operations using the unit commitment model, which could drastically increase the complexity of the problem. In fact, as the remote areas generally may have large difference between their peak and minimum demands, they may install low-load diesel generators or simply force thermal generators to work with light loads [1], for which it is not necessary to build the unit commitment model. Under this situation, we use a binary variable to model the working status of the local generator and to capture its fixed cost; a continuous variable is used to capture the variable generation cost.

Note that the role of a storage device is similar to that of a warehouse. It is used to store excess energy generated to meet future demands, along with just-in-time generation from the renewable energy and the local generator. One difference from classical inventory systems is that the energy loss from storage devices is often quite significant, as energy efficiency ranges from 60% (hydrogen storage) to 90% (battery storage). Although the energy loss can be high in storage devices, they are extremely useful to deal with randomness in renewable energy generation and demand.

In Figure 2(a), three daily demand curves are shown for three consecutive days (data from [17]). Figure 2(b) provides three daily wind speed curves for three consecutive days (data from [16]). From these figures, we see that the variability in hourly demand and wind speed cannot be ignored (particularly for wind speed), doing so could result in unmet demand or increased operating costs. Following the typical strategy in stochastic programming, every possible random situation is represented by a scenario with the associated probability. Specifically, because demand (or generation) could change dramatically over seasons, one year is decomposed into a set of "seasons," denoted by I, during which daily demands (or wind speed) are reasonably consistent. Then, each season can be represented by a single day. One possible demand curve (or wind curve) of a single day is represented by a scenario. The randomness of daily demand (or generation, respectively) is represented by S, a set of scenarios, and their associated discrete probabilities. Furthermore, for modeling operations of each energy component, a single day is divided into a set of time slots T (typically 24 slots for 24 hours). Typically, the system is designed such that for every season and in every scenario: (1) demand in all time slots must be be met by the sum of energy from various sources; (2) the "inventory level" in the storage device is balanced with respect to inflow and outflow and energy efficiency; (3) the production level of each component of the system must be less than or equal to the capacity of that component. Tables 1 and 2 summarize the parameters and variables use in the model to meet the objective.

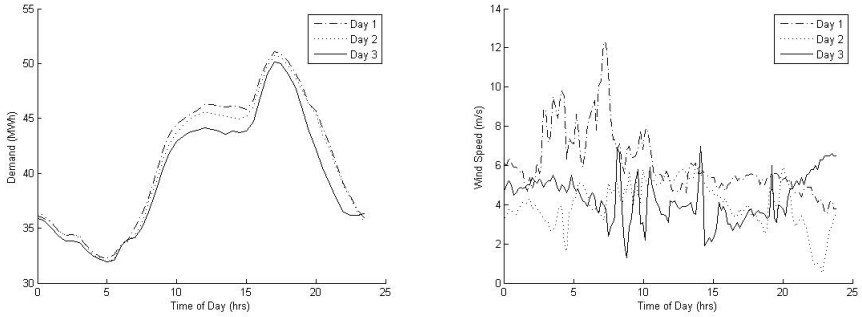

(a) Daily Demand Curves (b) Daily Wind Speed Curves

Figure 2: Daily Curves for Demand and Wind Speed

Table 1: Parameters for Model

C_w	cost of units of storage capacity
C_g	cost of each wind turbine
C_ℓ	cost of units of transmission line capacity
F_w	fixed cost associated with construction of a storage device
F_g	fixed cost associated with construction of a wind farm
F_ℓ	fixed cost associated with construction of a transmission line
C_k	cost associated with storage of energy per MW per time unit
C_p	cost per MWh of energy from transmission line
C_O	operating cost of local generation facility
K_w	size of capacity units of storage
$K_g(W)$	generation capacity of each wind turbine as a function of wind speed
K_ℓ	size of capacity units of transmission line
K_O	capacity of local generation facility
M_w	big-M constant for storage
M_g	big-M constant for wind turbines
M_ℓ	big-M constant for transmission line
P	length of planning horizon
s	element of S, the set of scenarios
i	element of I, the set of seasons
t	element of T, the set of time slots
γ	conversion factor for energy put into storage
β	conversion factor from cost of energy from transmission line to cost of energy from local generation

Table 2: Decision Variables for Model

w	number of storage capacity units purchased
g	number of wind turbines purchased
ℓ	number of transmission line capacity units purchased
x	1 if storage device is constructed
y	1 if wind turbines are erected
z	1 if transmission network is installed
$FO^s_{i,t}$	1 if local energy is used in (s,i,t)
$O^s_{i,t}$	amount of energy used to supply demand from local sources in (s,i,t)
$OS^s_{i,t}$	amount of energy put into storage from local sources in (s,i,t)
$S^s_{i,t}$	storage level in (s,i,t)
$SD^s_{i,t}$	amount of energy used to supply demand from storage in (s,i,t)
$L^s_{i,t}$	amount of energy used to supply demand from transmission line in (s,i,t)
$GS^s_{i,t}$	amount of energy put into storage from wind sources in (s,i,t)
$GD^s_{i,t}$	amount of energy used to supply demand from wind sources in (s,i,t)

Using these parameters and variables, the stochastic optimization model is formulated as follows:

$$\min \quad C_w w + C_g g + C_\ell \ell + F_w x + F_g y + F_\ell z + \\ + P\left[\mathbb{E}_s\left\{\sum_{i,t} C_k S^s_{i,t} + C_p L^s_{i,t} + C_O FO^s_{i,t} + \beta C_p\left(O^s_{i,t} + OS^s_{i,t}\right)\right\}\right] \tag{2.1}$$

subject to

$$D^s_{i,t} = L^s_{i,t} + GD^s_{i,t} + SD^s_{i,t} + O^s_{i,t} \quad s\in S,\ i\in I,\ t\in T \tag{2.2}$$
$$S^s_{i,t} = S^s_{i,t-1} + \gamma GS^s_{i,t} + \gamma OS^s_{i,t} - SD^s_{i,t} \quad s\in S,\ i\in I,\ t\in T \tag{2.3}$$
$$GS^s_{i,t} + GD^s_{i,t} \le K_g\left(W^s_{i,t}\right)\ g \quad s\in S,\ i\in I,\ t\in T \tag{2.4}$$
$$S^s_{i,t} \le K_w\, w \quad s\in S,\ i\in I,\ t\in T \tag{2.5}$$
$$L^s_{i,t} \le K_\ell\, \ell \quad s\in S,\ i\in I,\ t\in T \tag{2.6}$$
$$O^s_{i,t} + OS^s_{i,t} \le K_O\, FO^s_{i,t} \quad s\in S,\ i\in I,\ t\in T \tag{2.7}$$
$$w \le M_w\, x \tag{2.8}$$
$$g \le M_g\, y \tag{2.9}$$
$$\ell \le M_\ell\, z \tag{2.10}$$
$$O^s_{i,t},\ OS^s_{i,t},\ S^s_{i,t},\ SD^s_{i,t},\ L^s_{i,t}\ GS^s_{i,t}\ GD^s_{i,t} \in \mathbb{R}_+ \quad s\in S,\ i\in I,\ t\in T \tag{2.11}$$
$$FO^s_{i,t} \in \{0,1\} \quad s\in S,\ i\in I,\ t\in T \tag{2.12}$$
$$x,y,z \in \{0,1\} \tag{2.13}$$
$$w,g,\ell \in \mathbb{Z}_+ \tag{2.14}$$

The objective of the model is to minimize the sum of the building costs and expected operating costs over a given planning horizon P. There is a fixed cost associated with construction of a transmission line F_ℓ, a storage device F_w, and a wind farm F_g as well as an incremental cost per unit of each purchased C_ℓ, C_w, and C_g, respectively. The operating costs are the cost

of storage per MW per time unit in the storage device C_k, the cost per MWh of energy from the transmission line C_p, the fixed cost of operating the local energy source C_O, and the cost per MWh of energy from the local energy source which is captured as C_p multiplied by a factor β (typically $\beta \geq 1$). The expectation of these costs is taken over all scenarios in S. Adding the fixed costs with the expected value of the variable costs gives the objective function (2.1). Note that each scenario was weighted equally. For a sufficiently large number of scenarios, the true distribution will be approximated with little loss. Therefore, this is not an unreasonable assumption.

The first constraint (2.2) ensures the demand $D^s_{i,t}$ is met by the sum of the energy from the transmission line $L^s_{i,t}$, renewable energy $GD^s_{i,t}$, energy from storage $SD^s_{i,t}$, and energy from local sources $O^s_{i,t}$. The balance of the storage level $S^s_{i,t}$ with inflow, $\gamma GS^s_{i,t}$ and $\gamma OS^s_{i,t}$ and outflow relative to the previous level is guaranteed by (2.3). Note that two assumptions are made here: 1) the level in storage is already expressed in terms of dispatchable energy so that there is no loss in energy transfer from storage to the grid; 2) the discharge capacity of the storage device is equal to the capacity of the device. Constraint (2.4) gives the capacity for the total renewable energy used as a function of wind speed $K_g\left(W^s_{i,t}\right)$ and the number of wind turbines purchased g (in general, $K_g(-)$ is a function describing the output of the renewable energy system used). Figure 3 shows a typical wind power curve that defines the function $K_g(W)$. Notice that for a given wind speed, $K_g(W)$ is a constant. The storage level cannot exceed the number of storage units constructed w multiplied by the size of a storage capacity unit K_w, by (2.5). The amount of energy from the transmission line cannot exceed the number of transmission line units constructed ℓ multiplied by the capacity of a transmission line unit K_ℓ, by (2.6). $FO^s_{i,t}$ is a binary variable equal to 1 if the local generating facility is used in (s, i, t) and (2.7) ensures that local energy can be used only if the local energy production facility is operating at that time and the total usage cannot exceed the facility's capacity K_O. Additionally, x, y, and z are binary variables equal to 1 if construction of a storage device, a wind farm, or a transmission line occur, respectively, and zero otherwise. These are linked to w, g, and ℓ, respectively, through big-M constraints (2.8) - (2.10).

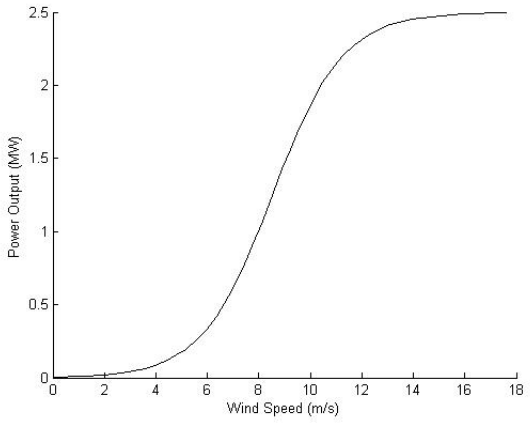

Figure 3: Wind Power Curve

Based on the role of the storage device in the whole system and the system flow balance dynamics, we observe that the whole model has a strong connection to the classical capacitated lot-sizing model [12]. In fact, we next show that the model, in its general form, has a structure of the capacitated lot-sizing model and therefore is difficult to solve.

Proposition 1. *The problem described by* (2.1)-(2.14) *is $\mathcal{NP}$-hard.*

Proof. We consider its simplest case where $|S| = 1$ and $|I| = 1$, i.e. a single scenario and a single season. When (i) the fixed cost of transmission line is very high, (ii) little renewable energy is available, (iii) both the fixed cost and unit cost of storage capacity are very low, it is clear that neither the transmission line will be built nor the green energy generation facility will be constructed while a sufficient storage device will be established. Therefore, the local generator will be the only generating source to meet demand. The original model is then reduced to

$$\begin{aligned}
\min \quad & C_w w + F_w y + P\left[\mathbb{E}_s\left\{\sum_{i,t} C_k S^s_{i,t} + C_O FO^s_{i,t} + \beta\left(C_p O^s_{i,t} + OS^s_{i,t}\right)\right\}\right] \\
\text{subject to} \quad & D^s_{i,t} = SD^s_{i,t} + O^s_{i,t} && (2.15)\\
& S^s_{i,t} = S^s_{i,t-1} + \gamma OS^s_{i,t} - SD^s_{i,t} && (2.16)\\
& O^s_{i,t} + OS^s_{i,t} \le K_O\, FO^s_{i,t} && (2.17)\\
& S^s_{i,t},\ SD^s_{i,t},\ O^s_{i,t},\ OS^s_{i,t} \in \mathbb{R}_+ && (2.18)\\
& w \in \mathbb{Z}^+, y \in \{0,1\} && (2.19)
\end{aligned}$$

Combining (2.15) and (2.16), we obtain

$$S^s_{i,t} + D^s_{i,t} = S^s_{i,t-1} + \gamma OS^s_{i,t} + O^s_{i,t},$$

which is exactly the flow balance equation in lot-sizing model if $\gamma = 1$. With the finite production capacity (2.17), this model is equivalent to the capacitated lot-sizing problem, which is known to be $\mathcal{NP}$-hard [12]. □

3 Solution Method

Given the structure of the problem defined by (2.1)-(2.14), we develop an algorithm using Benders' decomposition method [4], which is the most popular computation method in solving stochastic programming problems [3]. We first describe the decomposition scheme of our problem. Then, we introduce Pareto-optimal cuts and their integration into Benders' decomposition. Finally, we discuss performance improvement strategies and outline the algorithm implementation. To simplify our exposition, especially on the Pareto-optimal cuts, we do not give the scenario-wise primal and dual subproblem formulations although they can easily be obtained from the aggregated subproblem formulation.

3.1 Benders' Decomposition

Note that our model has a clear two stage structure: (i) in the system design stage, a small number of discrete decisions must be made, which are common to any seasons and stochastic scenarios; (ii) in the daily operation stage, many binary decisions for local generator and continuous flow variables must be determined given the realization of renewable energy generation. To take advantage of Benders' decomposition method and to balance the decomposed subsystems, we propose to incorporate all the local generator decisions as well as capacity variables into the first stage in the solution algorithm. Specifically, given values of w^*, g^*, ℓ^*, x^*, y^*, z^*, $\left(FO^s_{i,t}\right)^*$, $\left(O^s_{i,t}\right)^*$, and $\left(OS^s_{i,t}\right)^*$ satisfying (2.7) - (2.14) we can reduce the model defined by (2.1)-(2.14) to the following primal subproblem:

$$\min\ P\left[\mathbb{E}_s\left\{\sum_{i,t} C_k S^s_{i,t} + C_p L^s_{i,t}\right\}\right] \tag{3.1}$$

subject to

$$D^s_{i,t} \le L^s_{i,t} + GD^s_{i,t} + SD^s_{i,t} + \left(O^s_{i,t}\right)^* \quad s \in S,\ i \in I,\ t \in T \tag{3.2}$$

$$S^s_{i,t} \le S^s_{i,t-1} + \gamma GS^s_{i,t} + \gamma \left(OS^s_{i,t}\right)^* - SD^s_{i,t} \quad s \in S,\ i \in I,\ t \in T \tag{3.3}$$

$$GS^s_{i,t} + GD^s_{i,t} \le K_g \left(W^s_{i,t}\right)\ g^* \quad s \in S,\ i \in I,\ t \in T \tag{3.4}$$

$$S^s_{i,t} \le K_w\, w^* \quad s \in S,\ i \in I,\ t \in T \tag{3.5}$$

$$L^s_{i,t} \le K_\ell\, \ell^* \quad s \in S,\ i \in I,\ t \in T \tag{3.6}$$

$$S^s_{i,t},\ SD^s_{i,t},\ L^s_{i,t}\ GS^s_{i,t}\ GD^s_{i,t} \in \mathbb{R}_+ \quad s \in S,\ i \in I,\ t \in T \tag{3.7}$$

Let $\boldsymbol{\eta} = \{\eta^s_{i,t} \in \mathbb{R}_+ \ :\ s \in S,\ i \in I,\ t \in T\}$, $\boldsymbol{\lambda} = \{\lambda^s_{i,t} \in \mathbb{R}_+ \ :\ s \in S,\ i \in I,\ t \in T\}$, $\boldsymbol{\theta} = \{\theta^s_{i,t} \in \mathbb{R}_+ \ :\ s \in S,\ i \in I,\ t \in T\}$, $\boldsymbol{\delta} = \{\delta^s_{i,t} \in \mathbb{R}_+ \ :\ s \in S,\ i \in I,\ t \in T\}$, and $\boldsymbol{\alpha} = \{\alpha^s_{i,t} \in \mathbb{R}_+ \ :\ s \in S,\ i \in I,\ t \in T\}$ be the dual variables for constraints (3.2)-(3.6), respectively (assuming each constraint is rearranged to be of the form $\ge$, which can always be done). Then the dual of the primal subproblem, aptly named the dual subproblem, is formulated as:

$$\begin{aligned}\max \sum_{i,t,s} \big[&-\ell^* K_\ell \alpha^s_{i,t} - w^* K_w \delta^s_{i,t} - g^* K_g \left(W^s_{i,t}\right) \theta^s_{i,t} + \\ &+ \left(D^s_{i,t} - \left(O^s_{i,t}\right)^*\right) \eta^s_{i,t} - \gamma \left(OS^s_{i,t}\right)^* \lambda^s_{i,t} \big]\end{aligned} \tag{3.8}$$

subject to

$$\eta^s_{i,t} - \theta^s_{i,t} \le 0 \quad s \in S,\ i \in I,\ t \in T \tag{3.9}$$

$$\gamma\lambda^s_{i,t} - \theta^s_{i,t} \le 0 \quad s \in S,\ i \in I,\ t \in T \tag{3.10}$$

$$\lambda^s_{i,t+1} - \lambda^s_{i,t} - \delta^s_{i,t} \le PC_k \mathrm{Prob}\{s\} \quad s \in S,\ i \in I,\ t \in T \tag{3.11}$$

$$\eta^s_{i,t} - \lambda^s_{i,t} \le 0 \quad s \in S,\ i \in I,\ t \in T \tag{3.12}$$

$$\eta^s_{i,t} - \alpha^s_{i,t} \le PC_p \mathrm{Prob}\{s\} \quad s \in S,\ i \in I,\ t \in T \tag{3.13}$$

$$\alpha^s_{i,t}, \delta^s_{i,t}, \theta^s_{i,t}, \eta^s_{i,t}, \lambda^s_{i,t} \in \mathbb{R}_+ \quad s \in S,\ i \in I,\ t \in T \tag{3.14}$$

Notice that the feasible set for the dual subproblem, Ω, does not depend on the values of w^*, g^*, ℓ^*, x^*, y^*, z^*, $\left(FO^s_{i,t}\right)^*$, $\left(O^s_{i,t}\right)^*$, and $\left(OS^s_{i,t}\right)^*$. These values only affect the coefficients in the objective function of the dual subproblem.

Now the zero vector is in Ω, so the dual subproblem is always feasible though it may be unbounded. Therefore, the primal problem is either infeasible or feasible and bounded. Let P_Ω and R_Ω be the sets of extreme points and extreme rays of Ω, respectively. Then, the dual subproblem is bounded (and hence the primal subproblem is feasible and bounded) if

$$\begin{aligned}\sum_{i,t,s} \big[&-\ell^* K_\ell \alpha^s_{i,t} - w^* K_w \delta^s_{i,t} - g^* K_g \left(W^s_{i,t}\right) \theta^s_{i,t} + \\ &+ \left(D^s_{i,t} - \left(O^s_{i,t}\right)^*\right) \eta^s_{i,t} - \gamma \left(OS^s_{i,t}\right)^* \lambda^s_{i,t} \big] \le 0\end{aligned}$$

for all $(\boldsymbol{\eta}, \boldsymbol{\lambda}, \boldsymbol{\theta}, \boldsymbol{\delta}, \boldsymbol{\alpha}) \in R_\Omega$. Moreover, if both problems are feasible and bounded, then they have a common value of

$$\begin{aligned}\max_{(\eta,\lambda,\theta,\delta,\alpha)\in P_\Omega} \sum_{i,t,s} \big[&-\ell^* K_\ell \alpha^s_{i,t} - w^* K_w \delta^s_{i,t} - g^* K_g \left(W^s_{i,t}\right) \theta^s_{i,t} + \\ &+ \left(D^s_{i,t} - \left(O^s_{i,t}\right)^*\right) \eta^s_{i,t} - \gamma \left(OS^s_{i,t}\right)^* \lambda^s_{i,t} \big]\end{aligned}$$

Let ζ be a free variable, then the Benders' Master problem is formulated as:

$$\min C_w w + C_g g + C_\ell \ell + F_w x + F_g y + F_\ell z + \\ + P\left[\mathbb{E}_s\left\{\sum_{i,t} C_O FO^s_{i,t} + \beta C_p\left(O^s_{i,t} + OS^s_{i,t}\right)\right\}\right] + \zeta \tag{3.15}$$

subject to

$$\sum_{i,t,s}\left[-\ell K_\ell \alpha^s_{i,t} - wK_w\delta^s_{i,t} - gK_g\left(W^s_{i,t}\right)\theta^s_{i,t} + \right. \\ \left. + \left(D^s_{i,t} - O^s_{i,t}\right)\eta^s_{i,t} - \gamma OS^s_{i,t}\lambda^s_{i,t}\right] \le 0 \quad (\eta,\lambda,\theta,\delta,\alpha) \in R_\Omega \tag{3.16}$$

$$\zeta \ge \sum_{i,t,s}\left[-\ell K_\ell \alpha^s_{i,t} - wK_w\delta^s_{i,t} - gK_g\left(W^s_{i,t}\right)\theta^s_{i,t} + \right. \\ \left. + \left(D^s_{i,t} - O^s_{i,t}\right)\eta^s_{i,t} - \gamma OS^s_{i,t}\lambda^s_{i,t}\right] \quad (\eta,\lambda,\theta,\delta,\alpha) \in P_\Omega \tag{3.17}$$

$$O^s_{i,t} + OS^s_{i,t} \le K_O\, FO^s_{i,t} \quad s \in S,\ i \in I,\ t \in T \tag{3.18}$$

$$w \le M_w\, x \tag{3.19}$$

$$g \le M_g\, y \tag{3.20}$$

$$\ell \le M_\ell\, z \tag{3.21}$$

$$O^s_{i,t},\ OS^s_{i,t} \in \mathbb{R}_+ \quad s \in S,\ i \in I,\ t \in T \tag{3.22}$$

$$FO^s_{i,t} \in \{0,1\} \quad s \in S,\ i \in I,\ t \in T \tag{3.23}$$

$$x, y, z \in \{0,1\} \tag{3.24}$$

$$w, g, \ell \in \mathbb{Z}_+ \tag{3.25}$$

In general, this formulation can have a large number of constraints of the form (3.16) and (3.17), known as feasibility cuts and optimality cuts, respectively. A relaxed Benders' reformulation consists of replacing P_Ω and R_Ω with sets P'_Ω and R'_Ω in the Benders' Master problem such that $P'_\Omega \subset P_\Omega$ and $Q'_\Omega \subset Q_\Omega$. In [4], Benders describes an algorithm to iteratively add feasibility and optimality cuts to a relaxed Benders' reformulation for a mixed integer programming problem. The key initial observations for this algorithm are that an optimal solution to the relaxed Benders' reformulation provides a lower bound (LB) on the optimal value of the original problem and a solution to the relaxed Benders' reformulation provides values of w^*, g^*, ℓ^*, x^*, y^*, z^*, $\left(FO^s_{i,t}\right)^*$, $\left(O^s_{i,t}\right)^*$, and $\left(OS^s_{i,t}\right)^*$ satisfying (2.7) - (2.14) which serves as the input for the dual subproblem. Next, the dual subproblem is solved. If it has a finite optimal value, then an optimality cut can be added to the relaxed Benders' reformulation and an upper bound (UB) for the original problem can be found. If the dual subproblem is unbounded, then a feasibility cut can be added to the relaxed Benders' reformulation. Resolving the relaxed Benders' reformulation restarts the process. This continues until $LB = UB$, at which point an optimal solution has been found.

3.2 Pareto-Optimal Cuts

It is possible for the dual subproblem to have multiple optimal solutions. This can result in multiple optimality cuts, some of which are dominated. Additionally, if the dual subproblem is unbounded, there may be extreme rays which generate dominated cuts. Let $\Psi = (\boldsymbol{\eta}, \boldsymbol{\lambda}, \boldsymbol{\theta}, \boldsymbol{\delta}, \boldsymbol{\alpha}) \in P_\Omega \cup R_\Omega$ and $F(\Psi)$ denote the left hand side of (3.16), then we say Ψ dominates Ψ' if $F(\Psi) \ge F(\Psi')$ for all values of w, g, ℓ, x, y, z, $FO^s_{i,t}$, $O^s_{i,t}$, and $OS^s_{i,t}$ satisfying (2.7) - (2.14) and strict inequality holding for at least one point. A Pareto-optimal cut is one which is not

dominated by any other cut. Magnanti and Wong describe a method for generating Pareto-optimal cuts in [14]. It is done by first selecting a point, w^0, g^0, ℓ^0, x^0, y^0, z^0, $\left(FO^s_{i,t}\right)^0$, $\left(O^s_{i,t}\right)^0$, and $\left(OS^s_{i,t}\right)^0$, in the relative interior of the set defined by the linear relaxation of (2.7) - (2.14). Next, let obj^* be the objective function value of the dual subproblem solved using the point w^*, g^*, ℓ^*, x^*, y^*, z^*, $\left(FO^s_{i,t}\right)^*$, $\left(O^s_{i,t}\right)^*$, and $\left(OS^s_{i,t}\right)^*$, then the solution to the following problem defines a Pareto-optimal cut:

$$\max \sum_{i,t,s} \left[-\ell^0 K_\ell \alpha^s_{i,t} - w^0 K_w \delta^s_{i,t} - g^0 K_g \left(W^s_{i,t}\right) \theta^s_{i,t} + \right.$$
$$\left. + \left(D^s_{i,t} - \left(O^s_{i,t}\right)^0\right) \eta^s_{i,t} - \gamma \left(OS^s_{i,t}\right)^0 \lambda^s_{i,t}\right] \tag{3.26}$$

subject to

$$\eta^s_{i,t} - \theta^s_{i,t} \leq 0 \qquad s \in S,\ i \in I,\ t \in T \tag{3.27}$$
$$\gamma\lambda^s_{i,t} - \theta^s_{i,t} \leq 0 \qquad s \in S,\ i \in I,\ t \in T \tag{3.28}$$
$$\lambda^s_{i,t+1} - \lambda^s_{i,t} - \delta^s_{i,t} \leq PC_k \text{Prob}\{s\} \qquad s \in S,\ i \in I,\ t \in T \tag{3.29}$$
$$\eta^s_{i,t} - \lambda^s_{i,t} \leq 0 \qquad s \in S,\ i \in I,\ t \in T \tag{3.30}$$
$$\eta^s_{i,t} - \alpha^s_{i,t} \leq PC_p \text{Prob}\{s\} \qquad s \in S,\ i \in I,\ t \in T \tag{3.31}$$
$$\sum_{i,t,s} \left[-\ell^* K_\ell \alpha^s_{i,t} - w^* K_w \delta^s_{i,t} - g^* K_g \left(W^s_{i,t}\right) \theta^s_{i,t} + \right.$$
$$\left. + \left(D^s_{i,t} - \left(O^s_{i,t}\right)^*\right) \eta^s_{i,t} - \gamma \left(OS^s_{i,t}\right)^* \lambda^s_{i,t}\right] = obj^* \tag{3.32}$$
$$\alpha^s_{i,t}, \delta^s_{i,t}, \theta^s_{i,t}, \eta^s_{i,t}, \lambda^s_{i,t} \in \mathbb{R}_+ \qquad s \in S,\ i \in I,\ t \in T \tag{3.33}$$

Constraint (3.32) guarantees that the solution found has the same optimal value as the original point, and therefore it is in the original set of optimal solutions. If the dual subproblem is unbounded, obj^* may be replaced with a sufficiently large value. In our computational study, we observe that Pareto-optimal cuts have a significant impact on the computational performance.

3.3 Performance Improvement and Outline of the Algorithm

The two previous subsections describe the general idea behind the algorithm implemented in this paper. To further increase our algorithm's efficiency, we exploited the structure of our model to reduce the computational burden on solving master problems and subproblems.

First, because of the nature of stochastic programming, the dual subproblem defined in (3.8)-(3.14) is separable over scenarios, i.e. a dual subproblem for each scenario (DSP_s) can be solved independently. So, we make use of this property to generate multiple feasibility cuts in one iteration, i.e. if the objective function value is unbounded for any DSP_s, then a feasibility cut is added for each such s per iteration. When the objective function value is bounded for all DSP_s, we generate one optimality cut per iteration. Table 3 provides the pseudocode for the Benders' algorithm implemented in our work, which re-iterates this point.

Second, we obtain an initial feasible solution to the complete model by rounding its linear programming solution to a closest feasible solution [15]. Then, the partial solution for the master problem will be passed to the dual subproblem to generate feasibility cuts or an optimality cut of a high quality. Note also that its objective function value provides an upper bound.

Third, we observe that the master problem is a difficult mixed integer programming problem and any of its feasible solutions can be used to generate optimality and feasibility cuts.

As a result, we set a time limit on the computation of solving the Master problem for a set of iterations in the early stage. If the relaxed Master problem terminates before finding an optimal solution, the best solution found thus far is used for the subproblems.

Table 3: Pseudocode for Solution Algorithm

```
Solve the LP relaxation of the original problem and round integer
variables up to obtain a feasible solution for MP
WHILE relative gap greater than ϵ
    FOR s ∈ S
        Solve DSP_s
    IF DSP_s is bounded for all s ∈ S
        Solve Pareto subproblems for all s
        Add a single optimality cut to relaxed Master problem
    ELSE
        For each unbounded dual subproblem
            Solve Pareto subproblems for the bounded dual subproblem
            Add feasibility cut
```

4 Computational Study and Management Insights

4.1 Data Description

Demand data were collected from [17] and the wind data from [16]. The demand data used were specifically from England and Wales for 2009. The data were scaled down by a factor of 10^{-3}. The population of England and Wales is approximately 53M [20], so we have an estimated population of 53,000 for our rescaled demand data. Twelve seasons were used, one for each month. Scenarios were created by perturbing the observed data. A total of 55 datasets were created for numerical study. We summarize them into three categories based on their purpose. These categories are 1) comparison to professional solver, 2) impact of variance, and 3) impact of magnitude. Within each dataset, there are an equal number of demand and wind scenarios. This is indicated in the descriptions below by using the notation $a \times a$ for the total number of scenarios in a dataset. The datasets in each category are described forthwith:

- To compare the performance of our algorithm with a professional solver, 15 datasets of various sizes were generated. For demand scenarios, in a given time slot scenario data were generated from a normal distribution with mean equal to observed demand and standard deviation equal to 10 percent of the observed data. For the wind scenarios, in a given time slot the scenario data were generated by multiplying the observed wind speed by a random number drawn from a triangular distribution with parameters $(0.5, 1, 1.5)$. Within each dataset, an equal number of wind and demand scenarios were used. There are five datasets with 5×5 scenarios (S1-S5), five with 8×8 scenarios (M1-M5), and five with 11×11 scenarios (L1-L5). S, M, and L indicate small, medium, and large dataset sizes, respectively.
- To compare the system configuration in situations with different variance, another 20 datasets were generated, all with 8×8 scenarios. Five dataset (DV1-DV5) were generated similar to first 15, but with 25 percent rather than 10 percent for demand standard deviation followed by five datasets with 64 scenarios (LDV1-LDV5) with 5 percent

for demand standard deviation. Five datasets (WV1-WV5) were generated similar to the original 15 datasets, but with the parameters for the triangular distribution being $(0.25, 1, 1.75)$, then another five datasets (LWV1-LWV5) with triangular distribution parameters of $(0.75, 1, 1.25)$. DV and LDV indicate high demand variance and low demand variance, while WV and LWV indicate high wind variance and low wind variance.

- To evaluate the effect of rescaling the magnitude of wind and demand an additional 20 datasets with 8×8 scenarios were generated. Five datasets (TD1-TD5) were created by doubling original observed demand data and following the procedure for the original 15 datasets. Five datasets (TW1-TW5) were created by doubling original observed wind data and following the procedure for the original 15 datasets. Five datasets (HD1-HD5) were created by multiplying original observed demand data by one half and following the procedure for the original 15 datasets. Five datasets (HW1-HW5) were created by multiplying original observed wind data by one half and following the procedure for the original 15 datasets. TD and TW are datasets with twice demand and wind speed, respectively. HD and HW are datasets with half demand and wind speed, respectively.

The cost coefficients for our model were estimated based on information from engineers at a local utility company, as well as [23] and [24]. We describe the method by which they were determined here. A 600MW line was constructed from New Jersey to Long Island for \$600M, so to determine F_ℓ and C_ℓ we used this pricing information. Specifically, it was assumed that a 60 MW line (large enough for our demand data) would cost \$60M. Assuming 75% fixed cost and K_ℓ (the size of capacity units) is 20 MW, we have $F_\ell =$ \$45M and $C_\ell =$ \$5M. A number of storage devices were build in the United States for costs ranging from \$0.16M to \$0.65M per MW. Assuming the capacity is 200MW (large enough to store roughly three times the maximum demand) and the end cost is \$0.5M per MW, then using the same method as above with $K_w = 5$MW we have $F_w =$ \$75M and $C_w =$ \$0.625M. Finally, assuming a wind turbine's end cost is \$1.5M and that 250 turbines are purchased, then $F_g =$ \$280M and $C_g =$ \$0.38M. High fixed costs for storage and wind farm construction were used since we are considering pump storage, would require the construction of a reservoir, and an offshore wind farm, which also has considerable construction costs. The cost of storage C_k was set at \$0.1 per MW per hour in storage. We assumed the hourly operating cost of the local generating facilities C_O to be \$2000. The cost of energy in Tampa is \$100 per MWh, so this was the value used for C_p and energy from local sources was assumed to be three times as much ($\beta = 3$). The conversion factor for the energy placed into storage was taken to be 75% ($\gamma = 0.75$). Finally, K_O was set to be 75% of peak demand.

4.2 Traditional Benders' Decomposition Vs. Pareto-Optimal Cuts

To see the benefit of utilizing Pareto-optimal cuts in Benders' decomposition, the following experiment was conducted. The problem described by (2.1)-(2.14) with dataset M1 was solved using standard Benders' decomposition and Benders' with Pareto-optimal cuts. In Figure 4, the upper and lower bounds for both algorithms are depicted. This demonstrates using Pareto-optimal cuts can vastly reduce the computation time for this model as compared to traditional Benders'. Therefore, in all our computation experiments, we implement Pareto-optimal cuts within our Benders' decomposition algorithm.

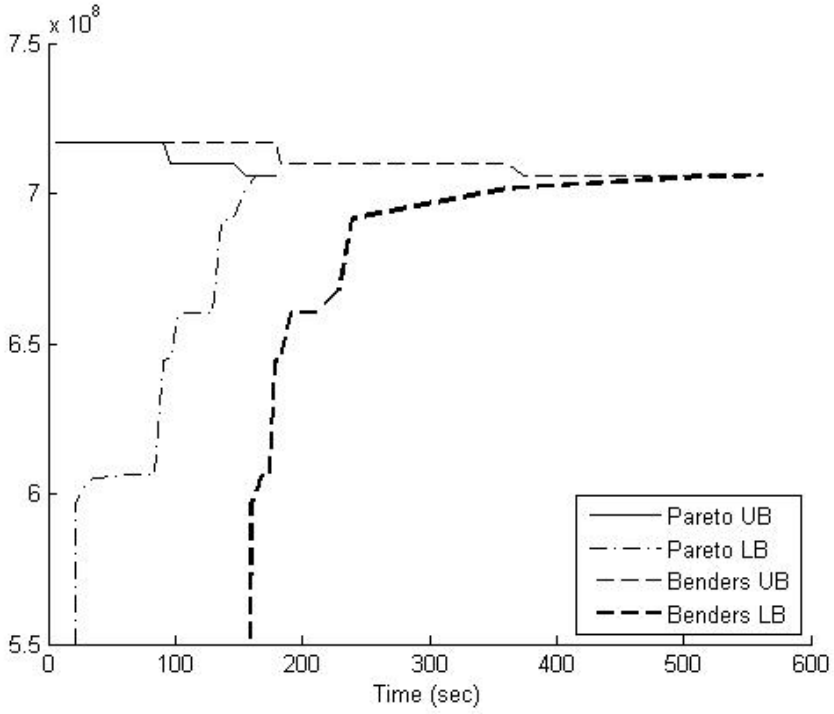

Figure 4: Bounds on Optimal Solution vs Time

4.3 Experimental Results

The problem described by (2.1)-(2.14) was solved with datasets S1-S5, M1-M5, and L1-L5 using Benders' decomposition with Pareto-optimal cuts (BD) and with a commercial solver. This was done on a computer running Windows 7 (64-bit) with a 3GHz processor and 4 GB of RAM. The solver used was Gurobi 3.0.3 (64-bit) [11], one of state-of-the-art solvers on the market, through Python 2.6.6. Table 4 summarizes the results of solving these 15 problems given the above configuration. Table 5 provides the average values of the results with respect to problem size. The percent gap is defined as $100(UB-LB)/LB$. The algorithm tolerance was set at 10^{-2} percent, which is the same value as Gurobi. We note that that Gurobi uses $100(UB-LB)/UB$ as default to define its percent gap, which is not the value given in Table 4, both % Gap columns are $100(UB-LB)/LB$. In general, it is true that $(UB-LB)/UB < (UB-LB)/LB$, so the gap utilized in our application of Benders' decomposition is stronger than Gurobi's. In all experiments, we set the computation time limit to 2 hours.

Table 4: Summary of Results

Dataset	BD % Gap	Gurobi % Gap	BD Time (sec.)	Gurobi Time (sec.)	BD Obj. Val.	Gurobi Obj. Val.
S1	0.008	0.009	117.05	100.73	706561567.07	706549940.33
S2	0.008	0.000	554.48	102.56	708043807.87	708043464.62
S3	0.006	0.000	81.77	507.13	703840113.46	703812904.63
S4	0.009	0.000	76.70	189.13	706328779.68	706309058.27
S5	0.008	0.000	633.46	125.38	702111074.33	702072593.27
M1	0.009	0.448	324.88	NA	705947550.58	705936734.97*
M2	0.007	0.000	342.58	7094.81	701129740.84	701128500.34
M3	0.008	0.000	864.09	5526.18	710631417.40	710613118.77
M4	0.009	0.010	441.97	5183.68	699700401.66	699696729.90
M5	0.008	0.005	645.02	1971.86	701073419.76	701073105.61
L1	0.008	36.489	1553.11	NA	702820002.70	714020536.27*
L2	0.009	36.607	1708.31	NA	706409914.25	716825714.19*
L3	0.009	36.338	1728.69	NA	704365041.50	715421887.79*
L4	0.009	35.562	2028.51	NA	705311891.95	708699790.44*
L5	0.008	35.924	1149.43	NA	704075375.96	716221101.22*

* indicates best value, not proven optimal
NA indicates time limit met

Table 5: Average Values of Results by Problem Size

Dataset Size	BD % Gap	Gurobi % Gap	BD Time (sec.)	Gurobi Time (sec.)	BD Obj. Val.	Gurobi Obj. Val.
S (5×5)	0.008	0.002	292.695	204.987	705377068.48	705357592.22
M (8×8)	0.008	0.004**	523.71	4944.13**	703696506.05	703689637.92
L (11×11)	0.009	36.184	1633.61	NA	704596445.27	714237805.98

** based on available 4 instances

For small instances (S1-S5) the commercial solver tended to outperform the algorithm, though their performances are comparable. However, we see that as the problem size grows the Benders' decomposition algorithm significantly outperforms Gurobi. For medium size instances with 8×8 scenarios, our algorithm generally is 10 times faster than Gurobi. For all large size instances with 11×11 scenarios, Gurobi fails to obtain an optimal solution within the 2 hour time limit. In fact, Gurobi fails to close the gap to a reasonable value in all large instances before its termination.

A variety of situations were considered to determine the model's sensitivity to the data. We first considered the effects of variance in wind speed and demand on the configuration of the system in the optimal solution. This was done through the use of datasets WV1-WV5, DV1-DV5, LWV1-LWV5, and LDV1-LDV5. The results are shown in Table 6. The columns of Table 6 are as following: g is the number of wind turbines, w is the number of storage capacity units (each unit is 5MW), ℓ is the number of transmission line capacity units (each unit is 20MW), Local refers to the total number of times local power sources were used across all

scenarios $\left(\text{Local } = \sum_{s,i,t} FO^s_{i,t}\right)$, Iterations is the number of iterations needed to terminate the algorithm, % Green is percentage of demand met from renewable energy, % Line is the percentage of demand met from the tranmission line, and % Local is the percentage of demand met by using localy generated energy. The percentage used in the last three columns is against all demand. For example, % Line is given by $\left(\sum_{s,i,t} L^s_{i,t}\right) / \left(\sum_{s,i,t} D^s_{i,t}\right)$, and the other two are computed similarly.

Table 6: Effect of Variance on System Configuration

Dataset	Obj. Val	g	w	ℓ	Local	Iterations	% Green	% Line	% Local
WV1	705527725.41	381	46	2	0	35	81.59	18.41	0.00
WV2	711511617.35	405	41	2	0	28	81.60	18.40	0.00
WV3	697302548.70	392	45	2	2	51	83.36	16.64	0.00
WV4	708697031.69	408	40	2	0	27	82.09	17.91	0.00
WV5	714025988.43	403	43	2	0	34	81.31	18.69	0.00
DV1	708677082.20	463	0	3	35	28	71.01	28.98	0.02
DV2	708982826.34	477	0	3	47	37	71.42	28.55	0.03
DV3	717128915.05	483	0	3	58	30	71.08	28.88	0.04
DV4	711149958.95	483	0	3	45	40	71.62	28.36	0.03
DV5	713026718.09	469	0	3	21	40	70.73	29.25	0.01
LWV1	691627990.06	476	0	3	0	24	74.07	25.93	0.00
LWV2	692151433.68	484	0	3	0	36	74.50	25.50	0.00
LWV3	692641808.91	479	0	3	0	24	74.16	25.84	0.00
LWV4	694487935.61	484	0	3	0	30	74.21	25.79	0.00
LWV5	692880099.81	473	0	3	0	31	73.83	26.17	0.00
LDV1	706712037.04	476	0	3	0	37	71.86	28.14	0.00
LDV2	707633350.59	463	0	3	0	31	70.92	29.08	0.00
LDV3	703016914.51	477	0	3	0	31	72.42	27.58	0.00
LDV4	703105451.39	464	0	3	0	38	71.67	28.33	0.00
LDV5	707166165.75	479	0	3	0	31	71.96	28.04	0.00
M1	705947550.58	473	0	3	0	27	71.73	28.27	0.00
M2	701129740.84	469	0	3	0	26	72.20	27.80	0.00
M3	710631417.40	480	0	3	0	29	71.48	28.52	0.00
M4	699700401.66	471	0	3	0	29	72.51	27.49	0.00
M5	701073419.76	482	0	3	0	29	73.07	26.93	0.00

There is little effect of variance on the optimal solution value, with the exception of low wind variance in which case the optimal value was lowered slightly. As shown in Table 7, the optimal configuration of system changes with variance. In particular, high wind variance lowers the number of wind turbines and capacity of the transmission line. This observation could be explained by the introduction of a storage device in the configuration of the system. As a direct result, the percentage of demand met by green energy is significantly higher than the other cases. This indicates that when there is enough wind at a higher speeds, it is worth while to store the excess energy. High variance in demand does not change the number of wind turbines much or the capacity of the transmission line. Additionally, the absence of a storage device remains unchanged. Interestingly, local energy production is utilized in the presence of

high demand variance. This indicates that the local generator will be used as the backup to mitigate the impact of variance. Overall, comparing variances in demand and wind, the latter one has more significant impact on system design.

Table 7: Average Values of Effect of Variance by Data Type

Dataset Type	Obj. Val	g	w	ℓ	Local	Iterations	% Green	% Line	% Local
WV	707412982.31	397.8	43.0	2.0	0.4	35.0	81.99	18.01	0.00
DV	711793100.12	475.0	0.0	3.0	41.2	35.0	71.17	28.80	0.02
LWV	692757853.61	479.2	0.0	3.0	0.0	29.0	74.15	25.85	0.00
LDV	705526783.86	471.8	0.0	3.0	0.0	33.6	71.77	28.23	0.00
M	703696506.05	475.0	0.0	3.0	0.0	28.0	72.20	27.80	0.00

Table 8: Effects of Rescaling on Optimal Solution

Dataset	Obj Val	g	w	ℓ	Local	Iterations	% Green	% Line	% Local
TW1	489395745.06	192	0	3	0	35	88.43	11.57	0.00
TW2	487139089.28	182	0	3	0	30	88.17	11.83	0.00
TW3	487344173.50	193	0	3	0	35	88.78	11.22	0.00
TW4	485744832.82	180	0	3	0	34	88.25	11.75	0.00
TW5	489631540.76	193	0	3	0	35	88.44	11.56	0.00
TD1	1025436900.65	799	86	4	0	51	81.27	18.73	0.00
TD2	1026794803.22	822	80	4	0	41	81.61	18.39	0.00
TD3	1018080831.46	779	80	4	0	55	80.93	19.07	0.00
TD4	1021445436.95	825	79	4	0	53	81.99	18.01	0.00
TD5	1032063058.80	849	76	4	0	44	81.74	18.26	0.00
HW1	724589905.39	0	0	3	176	10	0.00	99.90	0.10
HW2	720368367.77	0	0	3	80	7	0.00	99.96	0.04
HW3	722067291.05	0	0	3	152	16	0.00	99.95	0.05
HW4	724059893.31	0	0	3	160	15	0.00	99.95	0.05
HW5	726309583.98	0	0	3	168	11	0.00	99.95	0.05
HD1	385781244.25	0	0	2	0	4	0.00	100.00	0.00
HD2	385084899.26	0	0	2	0	3	0.00	100.00	0.00
HD3	383586693.10	0	0	2	0	4	0.00	100.00	0.00
HD4	385436764.32	0	0	2	0	4	0.00	100.00	0.00
HD5	384947960.05	0	0	2	0	3	0.00	100.00	0.00
M1	705947550.58	473	0	3	0	27	71.73	28.27	0.00
M2	701129740.84	469	0	3	0	26	72.20	27.80	0.00
M3	710631417.40	480	0	3	0	29	71.48	28.52	0.00
M4	699700401.66	471	0	3	0	29	72.51	27.49	0.00
M5	701073419.76	482	0	3	0	29	73.07	26.93	0.00

Datasets TW1-TW5, TD1-TD5, HW1-HW5, and HD1-HD5 were used to examine the effects of rescaling the demand data and wind speed data on the optimal configuration of the

energy system. Table 8 shows the results of these trials, and Table 9 provides the average values with respect to dataset type. Doubling the initial wind speed data results in a significant cost savings and reduces the number of wind turbines by a factor of about 2.5; no other values in the optimal configuration are changed. Doubling the initial demand data nearly doubles the number of wind turbines, induces a significant amount of energy storage, and increases the capacity of the transmission line. When demand is low, the transmission line could provide an economic advantage. Nevertheless, with demand increases, renewable energy generation facilities combined with the storage devices will become economically beneficial. In fact, this benefit is clearer as demand increases.

Table 9: Average Values of Effect of Rescaling by Data Type

Dataset Type	Obj. Val	g	w	ℓ	Local	Iterations	% Green	% Line	% Local
TW	487851076.28	188.0	0.0	3.0	0.0	33.8	88.42	11.58	0.00
TD	1024764206.22	814.8	80.2	4.0	0.0	48.8	81.51	18.49	0.00
HW	723479008.30	0.0	0.0	3.0	147.2	11.8	0.00	99.94	0.06
HD	384967512.20	0.0	0.0	2.0	0.0	3.6	0.00	100.00	0.00
M	703696506.05	475.0	0.0	3.0	0.0	28.0	72.20	27.80	0.00

Finally, the numerical study shows that the changes in the magnitudes of wind or demand changes the computational complexity as well. The larger the magnitude of demand (or wind), the larger the number of Benders' iterations required.

4.4 Additional Insights

It is to be expected that the yearly average wind speed could provide some insight to the expected number of wind turbines to purchase (if any). To explore this, wind scenarios were eliminated from dataset M1. The wind in every time slot was then replaced with values ranging from 1 to 18 for every season and scenario. The problem defined by (2.1)-(2.14) was solved for each wind speed from 1 to 18. Figure 5(a) shows the number of wind turbines purchased in the optimal solution versus wind speed. In Figure 5(b), the percent of green, line, and local energy (as defined in section 4.3) in the optimal solution are given as a function of wind speed. These figures indicate there is a critical wind speed that determines whether wind turbines are purchased. Additionally, there is a transition from energy delivered by the transmission line to energy delivered by the wind farm.

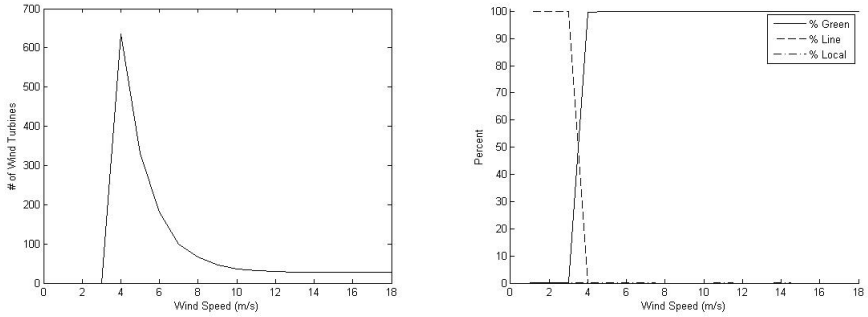

(a) Number of Wind Turbines vs. Wind Speed

(b) % Generation vs. Wind Speed

Figure 5: Effects of Average Wind Speed on Optimal Solution

5 Conclusions

In this paper, we developed a stochastic mixed integer programming model to determine the optimal configuration of a hybrid system consisting of a renewable energy facility, storage device, long distance transmission lines, and a local energy facility. Additionally, an efficient algorithm utilizing Benders' decomposition was created. It was found that the algorithm outperforms a solver (Gurobi) consistently for moderate and large sized problems, and performs comparably for small size instances. Although the model was applied to wind energy, it is applicable to other forms of renewable energy such as solar and tides. To the best of our knowledge, this is the first time that the comprehensive hybrid system configuration problem is modeled by a stochastic integer program and solved by an efficient algorithm. Possible areas for future work include expanding the model to consider multiple renewable sources simultaneously, unit commitment problem for local generator(s), and allowing construction at different times in the planning horizon along with associated lead times.

6 Acknowledgments

The authors wish to thank Mr. Adam Parke and Mr. Gordon Gillette at Tampa Electric Company for their support to this work.

References

[1] C. Abbey and G. Joos, "A stochastic optimization approach to rating of energy storage systems in wind-diesel isolated grids", in *Power Systems, IEEE Transactions on*, Vo. 24, No.1, pp. 418–426, 2009.

[2] J.P. Barton and D.G. Infield, "Energy Storage and Its Use with Intermittent Renewable Energy," in *IEEE Transactions on Energy Conversion*, Vol. 19, No. 2, pp. 441-448, June 2004.

[3] J.R. Birge and F. Louveaux, *Introduction to stochastic programming*, 2004. Springer Verlag.

[4] J.F. Benders, "Partitioning Procedures for Solving Mixed-Variables Programming Problems," in *Computational Management Science*, Vol. 2, pp. 3-19, 2005

[5] J.L. Bernal-Agustín and R. Dufo-López, "Simulation and optimization of stand-alone hybrid renewable energy systems," in *Renewable and Sustainable Energy Reviews*, Vo. 13, No. 8, pp. 2111–2118, 2009.

[6] P.D. Brown, J.A.P. Lopes, and M.A. Matos, "Optimization of Pumped Storage Capacity in an Isolated Power System with Large Renewable Penetration," in *IEEE Transactions on Power Systems*, Vol. 23, No. 2, pp. 523-531, May 2008

[7] N. Duic and M.d.G. Carvalho, "Increasing renewable energy sources in island energy supply: case study Porto Santo," in *Renewable and Sustainable Energy Reviews*, Vol. 8, No. 4, pp. 383-399, 2004

[8] O. Ekren and B.Y. Ekren, "Size optimization of a PV/wind hybrid energy conversion system with battery storage using simulated annealing," in *Applied Energy*, Vo. 87, No. 2, pp. 592–598, 2010

[9] General Algebraic Modeling System, `www.gams.com`

[10] GovTrack, `www.govtrack.us/congress/bill.xpd?bill=h111-2454`

[11] Gurobi Optimization, `www.gurobi.com`

[12] B. Karimi, S.M.T. Fatemi Ghomi, and J.M. Wilson, "The Capacited Lot Sizing Problem: A Review of Models and Algorithms," in *Omega - The International Journal of Management Science*, Vol. 31, pp. 365-378, 2003

[13] Y.Katsigiannis and P. Georgilakis, "Optimal sizing of small isolated hybrid power systems using tabu search", in *Journal Of Optoelectronics And Advanced Materials*, Vol.10, No. 5, pp. 1241–1245, 2008

[14] T.L. Magnanti and R.T. Wong, "Accelerating Benders' Decomposition: Algorithmic Enhancement and Model Selection Criteria," in *Operations Research*, Vol. 29, No. 3, pp. 464-484, 1981

[15] G. Nemhauser and L. Wolsey, Integer and Combinatorial Optimization, Wiley-interscience. 1988.

[16] National Climatic Data Center, `www.ncdc.noaa.gov`

[17] National Grid: The Power of Action, `www.nationalgrid.com`

[18] P. Nema, RK. Nema and S. Rangnekar, "A current and future state of art development of hybrid energy system using wind and PV-solar: A review," in *Renewable and Sustainable Energy Reviews*, Vol. 13, No.8, pp. 2096–2103, 2009.

[19] E.M. Nfah, J.M. Ngundam and R. Tchinda, "Modelling of solar/diesel/battery hybrid power systems for far-north Cameroon," in *Renewable Energy*, Vol.32, No. 5, pp. 832–844, 2007.

[20] Office for National Statistics, `http://www.statistics.gov.uk/CCI/nugget.asp?ID=6`

[21] S. Pereira, R. Segurado, A. Costa, A. Pipio, L. Alves, "Energy Storage and Its Use with Intermittent Renewable Energy," in *Chemical Engineering Transactions*, Vol. 18, pp. 629-634, 2009.

[22] T. Senjyu, D. Hayashi, A. Yona, N. Urasaki, and T. Funabashi, "Optimal Configuration of Power Generating Systems in Isolated Island with Renewable Energy," in *Renewable Energy*, Vol. 32, pp. 1917-1933, 2007

[23] Symbiotics: A New Generation of Hydropower, `www.symbioticsenergy.com/`

[24] Wind Power: Wind Power for Every Home, `www.mywindpowersystem.com/`